APPLICATION AND PERFORMANCE OPTIMIZATION OF PHASE CHANGE ENERGY STORAGE MATERIALS IN ROAD ASPHALT MIXTURES

by

Jiyao JIA[a], Xianjun WU[b], Sili LI[b], Dongsheng SUN[b], Liangjiajing DENG[c*], and Zhi ZHOU[d]

[a] Hubei Changjiang Road and Bridge Co., Ltd, Wuhan, China
[b] Hubei Communications Investment Construction Group Co., Ltd, Wuhan, China
[c] School of Economics and Management, China University of Geosciences, Wuhan, China
[d] Business School, Hubei University of Economics, Wuhan, China

Original scientific paper
https://doi.org/10.2298/TSCI2506187J

Application and performance optimization of phase change energy storage materials for road asphalt mixtures are investigated. A thermal-mechanical coupling prediction algorithm (HTCPPO) is proposed. It was found that the phase change temperature was 25-40 ℃, average potential heat was 180 J/g, and 15 ℃ temperature was 1.2 W/mK. After the algorithm simulation, the performance is optimal when the dosage is 10%. The internal temperature change decreases by 35% when the ambient temperature changes by 10 ℃, the compressive strength reaches 12 MPa (an increase of 20%), and the Marshall stability increases by 25% to 8 kN. The algorithm achieves precise optimization and provides a new technical path for road engineering.

Key words*: phase change energy storage materials, road asphalt mixture, HTCPPO algorithm, performance optimization, thermal-mechanical coupling*

Introduction

In road engineering, the performance of asphalt mixture is significantly affected by temperature. High temperatures in summer reduce its deformation resistance. When the road surface temperature exceeds 60 ℃ at noon in the south, heavy vehicles rolling over it easily produce ruts of more than 5 cm, which affects safety. Low temperatures in winter cause brittle cracking of materials. When the road surface temperature is minus 20 ℃ in the north, cracks in the road surface accelerate the damage to the base layer. The maintenance cost of temperature-related diseases accounts for more than 40% of the total maintenance cost, seriously affecting traffic efficiency [1].

Phase change energy storage materials have attracted attention due to their temperature regulation characteristics. They absorb and release a large amount of latent heat during phase change, which can stabilize the temperature of the mixture. High temperature absorption delays the temperature rise, and low temperature release slows down cooling [2]. For example, paraffin-based materials can achieve high temperature cooling of 5-8 ℃ and low temperature cooling

* Corresponding author, e-mail: liangjiajingdeng@gmail.com

of 3-4 ℃, which is expected to improve road stability. However, in practical applications, the compatibility and long-term stability of materials and mixtures still require further study, and the leakage issue of some materials after multiple phase changes needs to be addressed [3].

The fusion of machine learning and thermodynamics presents a new avenue for research, as machine learning can accurately predict performance (error ≤5%) and thermodynamics reveals the underlying energy mechanisms. The combination of the two can improve efficiency and deepen cognition. This study will explore the optimal application mode of PCM, optimize the comprehensive performance of the mixture, establish a referenceable methodology by building a predictive model, promote interdisciplinary innovation, and provide support for enhancing the performance of road projects.

Analysis of thermodynamic properties of phase change energy storage materials and road asphalt mixtures

Determination of thermodynamic parameters of phase change energy storage materials

Test methods for key parameters such as phase change temperature and phase change latent heat

In this paper, Netzsch DSC 214 instrument (temperature range –150-700 ℃, precision: ±0.1 ℃) was used to measure phase change energy storage material parameters by DSC. After grinding the sample to powder (5-10 mg), loading it in aluminum crucible with empty crucible as reference. Under the protection of nitrogen, the temperature of 5 °C per minute, 10 °C per minute, and 15 °C per minute were increased and decreased, three times [4].

In data processing, to accurately calculate the latent heat of phase change, considering the influence of heating rate on the test results, a correction formula is introduced:

$$Q = \int_{T_1}^{T_2} \left(C_p - k\beta \right) \mathrm{d}T \tag{1}$$

where Q [Jg^{-1}] is the corrected latent heat of phase change, C_p [Jg^{-1}°C^{-1}] – the specific heat capacity of the sample, k – the rate correction coefficient (obtained through multiple experimental fittings, with a value range of 0.02~0.05), β [°C per minute] – the heating rate, and T_1, T_2 [°C] – the start temperature and end temperature, respectively [5].

A tangency method is used to determine the temperature of phase change in which the temperature at the inflection point of the DSC curve is called phase change temperature [6]. In addition, in order to reduce system error, this paper introduces temperature correction equation:

$$T_{\mathrm{corr}} = T_{\mathrm{meas}} + \alpha \left(T_{\mathrm{meas}} - T_{\mathrm{ref}} \right) \tag{2}$$

where T_{corr} [°C] is the corrected phase change temperature, T_{meas} [°C] – the measured temperature, T_{ref} [°C] – the known phase change temperature of the standard substance (such as indium) and α – the temperature correction coefficient (obtained from the standard substance calibration experiment, about 0.003).

Comparison of thermodynamic properties of different types of phase change energy storage materials

Three PCM – paraffin (C18-C24), fatty acid (stearic-palmitic), PEG4000 – were compared via DSC: their phase transition temps, latent heats, and thermal conductivities are 28-32 °C/180-200 J/g/0.20-0.25, 25-28 °C/170-190 J/g/0.18-0.22, 38-42 °C/160-180 J/g/0.22-0.26 W/mK, respectively.

To comprehensively evaluate its applicability in road asphalt mixture, a comprehensive evaluation index of thermodynamic properties, I, was constructed [7]:

$$I = 0.4\frac{\Delta H}{\Delta H_{\max}} + 0.3\frac{T_{\mathrm{p}} - T_{\mathrm{amb}}}{T_{\max} - T_{\mathrm{amb}}} + 0.3\frac{\lambda}{\lambda_{\max}} \tag{3}$$

where ΔH is the potential heat of phase transformation, $\Delta H_{\max}$ – the maximal potential heat of phase transition, T_{p} – the variation of phase, T_{amb} – the yearly mean of the ground surface temperature, $T_{\max}$ – the peak temperature of the three materials, λ – the heat conduction, and $\lambda_{\max}$ – the largest thermal conductivity. It was found that paraffin $I = 0.82$, fatty acid $I = 0.76$, polyethylene glycol $I = 0.71$, which suggested that wax was better suited to the research situation [8].

Study on the thermodynamic properties of road asphalt mixture

Determination of parameters such as thermal conductivity and specific heat

According to the heat conduction theory, the thermal conductivity coefficient, λ, is calculated:

$$\lambda = \frac{Q}{4\pi\Delta T}\ln\left(\frac{t_2}{t_1}\right) \tag{4}$$

where Q [Wm^{-1}] is the heating power per unit length of the hot wire, ΔT [°C] – the temperature difference between t_1 and t_2, and t_1, t_2 [s] – the heating times, where $t_2 > t_1$.

In order to correct the effect of aggregate on the specific heat capacity of the mixture, a formula for calculating the specific heat capacity of the mixture is introduced:

$$c_{\mathrm{mix}} = \phi_{\mathrm{a}} c_{\mathrm{a}} + \phi_{\mathrm{a}} c_{\mathrm{p}} + \left(1 - \phi_{\mathrm{a}} - \phi_{\mathrm{p}}\right) c_{\mathrm{ag}} \tag{5}$$

where c_{mix} [Jkg^{-1}°C^{-1}] is the specific thermal capacity of asphalt mixture ϕ_{a} – the bulk fraction of asphalt, c_{a} – the specific thermal capacity of asphalt, ϕ_{p} – the bulk fraction of the phase-change substance, c_{p} – is the thermal capacity of the phase-change material, and c_{ag} – the specific thermal capacity of the aggregate [9].

Effect of temperature change on the mechanical properties of asphalt mixture

In this paper, the mechanical properties of asphalt mixtures at different temperatures (–10 °C, 0 °C, 20 °C, 40 °C, 60 °C) have been investigated. Compression strength tests were carried out with material testing system (MTS810), 100 mm × 100 mm × 100 mm, loading rate 1 mm per minute. Bending strength test was performed by a three points bending method, 40 mm × 40 mm × 160 mm, 100 mm span, and 5 mm per minute loading rate, Marshall stability test was performed according to JTG E20-2011 Specification [10]. It is found that the influence of temperature on the mechanical performance is remarkable, and the thermal strength relation model is established:

$$\sigma(T) = \sigma_{20}\mathrm{e}^{-k_1(T-20)} + \sigma_{\min}\left(1 - \mathrm{e}^{-k_2(T-20)}\right) \tag{6}$$

where $\sigma(T)$ [MPa] is the strength at temperature T, σ_{20} – the strength at 20 °C, $\sigma_{\min}$ – the high temperature ultimate strength, and k_1, k_2 – the temperature sensitivity coefficients (through experimental data fitting, compressive strength $k_1 = 0.035$, $k_2 = 0.021$).

Thermodynamic analysis of compatibility between phase change energy storage materials and asphalt mixtures

Calculation and analysis of interface binding energy

Molecular dynamics simulation is used to calculate the interface binding energy, and a phase change material-asphalt interface model is constructed [11]. The calculation formula of interface binding energy, E_{ad} is:

$$E_{ad} = \frac{E_{total} - E_{PCM} - E_{asphalt}}{A} \tag{7}$$

where E_{total} [eV] is the total energy of the interface system, E_{PCM} – the energy of the PCM when it exists alone, $E_{asphalt}$ – the energy of asphalt when it exists alone, and A – the interface area [Å^2]. The calculated paraffin-asphalt interface binding energy is –0.052 eV/ Å^2. The larger the absolute value, the better the compatibility.

Study on the thermodynamic stability of the mixed system

From a thermodynamic point of view, the Gibbs free energy change ΔG_{mix} of the mixed system:

$$\Delta G_{mix} = \Delta H_{mix} - T\Delta S_{mix} \tag{8}$$

where ΔH_{mix} is the mixing enthalpy and ΔS_{mix} – the mixing entropy. For a polymer-small molecule mixed system,

$$\Delta H_{mix} = \chi \mathrm{R} T \phi (1-\phi)$$

where χ is the Flory-Huggins interaction parameter and ϕ – the volume fraction of the PCM,

$$\Delta S_{mix} = -R\left[\phi \ln\phi + (1-\phi)\ln(1-\phi)\right]$$

Thermo-mechanical coupling performance prediction and optimization algorithm (HTCPPO algorithm)

Algorithm design ideas

Combining thermodynamic principles to build a theoretical model of material performance

The core theoretical basis of the HTCPPO algorithm comes from the conservation of thermodynamic energy and the thermo-mechanical coupling effect. For the phase change energy storage asphalt mixture system, an energy balance equation including the phase change latent heat release/absorption is constructed:

$$\rho c_p \frac{\partial T}{\partial t} = \nabla(\lambda \nabla T) + \rho_p L \frac{\partial \alpha}{\partial t} + \beta\sigma : \dot{\varepsilon} \tag{9}$$

where ρ [kgm^{-3}] is the density of the mixture, c_p [Jkg^{-1}K^{-1}] – the specific heat capacity T [K] – the temperature, t [s] – the time, λ [Wm^{-1}K^{-1}] – the thermal conductivity, ρ_p [kgm^{-3}] – the density of the PCM, L [Jkg^{-1}] – the latent heat of phase change, α – the phase change conversion rate ($0 \le \alpha \le 1$), β [Pa^{-1}] – the thermal-mechanical coupling coefficient σ [Pa] – the stress tensor, and $\dot{\varepsilon}$ [s^{-1}] – the strain rate tensor. The momentum balance equation introduces the temperature strain term:

$$\nabla\sigma + \rho \mathrm{g} = \rho \ddot{i} \tag{10}$$

where

$$\sigma = D:\left(\varepsilon - \varepsilon_T\right),\ \varepsilon_T = \alpha_T\left(T - T_0\right)I$$

D [Pa] is the elastic matrix, ε – the total strain tensor, ε_T – the temperature strain tensor, α_T [K^{-1}] – the thermal expansion coefficient, T_0 [K] – the reference temperature, I – the unit tensor, g [ms^{-2}] – the gravitational acceleration, $\ddot{u}$ [ms^{-2}] – the acceleration vector. By coupling these two equations, the interaction between temperature field and stress field can be characterized.

Using machine learning to process experimental data and optimize model parameters

Machine learning optimizes hard-to-quantify thermodynamic parameters using 3000 datasets with varying doping, temperatures (–10-60 °C), stresses (0-5 MPa), and thermal-mechanical data. Design parameter optimization objective function:

$$J(\theta) = \frac{1}{N}\sum_{i=1}^{N}\left[y_i - \hat{y}_i(\theta)\right]^2 + \lambda\sum_{k=1}^{M}\left|C_k(\theta)\right| \tag{11}$$

where θ is the parameter vector to be optimized, N – the number of samples, y_i – the measured value, $\hat{y}_i$ – the predicted value, λ – the constraint penalty coefficient, M – the number of thermodynamic constraints, and C_k – the k constraint (such as energy conservation deviation).

Algorithm structure composition

Data input layer

The input layer contains three types of characteristic parameters: phase change energy storage material parameters (phase shift temperature, T_m, phase change latent heat, L, thermal conductivity, λ_p, dosage, ϕ, *etc.*), asphalt mixture parameters (gradation fractal dimension, D_f, asphalt-stone ratio, ω, aggregate elastic modulus, E_a, *etc.*), and environmental parameters (solar radiation intensity, Q_s, wind speed, v, initial temperature, T_0, *etc.*). To eliminate the difference in parameter magnitude, the improved standardization formula is used:

$$x' = \frac{x - \mu_x}{\sigma_x + \epsilon}\left(\frac{\sigma_x}{\epsilon}\right) \tag{12}$$

where μ_x is the mean, σ_x – the standard deviation, and $\epsilon = 10^{-6}$ – the correction term to prevent the denominator from being zero.

Feature extraction layer

Based on the heat conduction equation and the stress-strain relationship, six core feature variables are extracted:

Temperature gradient amplitude,

$$G_T = \left\|\nabla T\right\|\ \left[\mathrm{Km}^{-1}\right]$$

reflecting the driving force of heat conduction. Heat flux vector $q = -\lambda\nabla T$ W/m^2 characterizing the intensity of heat transfer. Phase change completion

$$\alpha = \int_{T_{\text{start}}}^{T}\frac{1}{T_{\text{end}} - T_{\text{start}}}\mathrm{d}T$$

where dT describing the phase change process. Equivalent elastic modulus

$$E_{\text{eq}} = E_0 \exp\left[-k_1\left(T - T_0\right) - k_2\alpha\right]$$

reflecting the synergistic effect of temperature and phase change. Thermal stress factor

$$\sigma_T = E_{\text{eq}}\alpha_T\left(T - T_0\right) \text{ [MPa]}$$

quantifying the internal stress caused by temperature. Damage accumulation

$$D = \int_0^t \dot{\varepsilon}_{\text{pl}} \exp\left(-\frac{\sigma}{\sigma_0}\right) \mathrm{d}t$$

evaluates the degree of material degradation.

The feature extraction process uses a method combining principal component analysis with thermodynamic weights, and the feature contribution formula:

$$w_i = \frac{\text{Cov}\left(f_i, y\right)\exp\left[-\text{Dev}\left(f_i, C\right)\right]}{\sum_{j=1}^{6}\text{Cov}\left(f_j, y\right)\exp\left[-\text{Dev}\left(f_i, C\right)\right]} \tag{13}$$

where Cov is the covariance and Dev – the deviation between the feature and the thermodynamic constraint, which enables adaptive screening of key features, reducing the input dimension by 62% while retaining 91% of the information entropy.

Model training layer

The improved deep belief network (DBN) is used as the training subject, comprising three restricted Boltzmann machine (RBM) layers (with 64 nodes, 32 nodes, and 16 nodes, respectively) and one fully connected output layer. During the training process, the thermodynamic constraints are embedded, and the loss function with constraint terms is designed:

$$\mathcal{L} = \mathcal{L}_{\text{MSE}} + \gamma\sum_{k=1}^{3}\max\left(0, C_k\right) \tag{14}$$

where $\mathcal{L}_{\text{MSE}}$ is the mean square error loss, $\gamma = 10$ – the penalty coefficient, $C_1 = |Q_{\text{in}} - Q_{\text{out}} - \text{Q}_{\text{pc}}|$ – the energy conservation deviation, $C_2 = \max(0, \dot{S}_{\text{total}})$ – the entropy increase principle constraint, and $C_3 = |\sigma_{\text{pred}} - \sigma_{\text{thermo}}|$ – the stress consistency deviation.

Prediction output layer

The output layer can output two types of results at the same time: thermal-mechanical performance indicators (temperature field distribution, $T(x, y, z, t)$ maximum compressive stress, $\sigma_{\max}$, cumulative plastic strain, $\varepsilon_{\text{pl,acc}}$, *etc.*) and optimization scheme (optimal dosage range $[\phi_{\min}, \phi_{\max}]$ and performance improvement rate, η).

To achieve multi-objective optimization, a comprehensive performance evaluation function is constructed:

$$F = \omega_1\frac{\Delta T}{\Delta T_{\text{ref}}} + \omega_2\frac{\sigma_{\max}}{\sigma_{\text{ref}}} + \omega_3\frac{1}{1+\phi c_p} \tag{15}$$

where $\omega_1 = 0.4$, $\omega_2 = 0.4$, and $\omega_3 = 0.2$ are weight coefficients, ΔT – the temperature adjustment range, ΔT_{ref} – the reference value, σ_{ref} – the standard strength, and c_p [¥/kg] – the unit price of phase change material.

Experimental design

Data set construction

The dataset is divided into 3240 pre-processed datasets (2268, including full doping and temperature gradient), a validation set (324, including untrained 5% humidity variables), and a test set (648, including 12% doping extreme conditions) in a ratio of 7:1:2 [12]. Stratified sampling is used to ensure that the distribution of parameters within each subset is consistent with the distribution of parameters in the original dataset. For example, the doping ratio of phase change materials is maintained at 0%, 5%, 8%, 10%, and 12% at 14193 : 1 : 1 : 1 : 1, and the temperature range spans from –10-60 ℃ to minimize model deviation caused by data offset.

Feature engineering selects 12 core features based on mutual information entropy, performs polynomial transformations on non-linear features, introduces interactive features, and reduces the dimension from 38 to 12 through principal component analysis, retaining 96.3% of the information entropy. Kernel density estimation verifies the consistency of data distribution.

Algorithm training process

In this algorithm, a loss function is adopted, which is a combination of weighted ANOVA and thermodynamic constraints, and the weight coefficient is adjusted dynamically. The optimizer uses an Adam algorithm, with a learning rate of 0.001, a decay strategy, and a batch size of 32, and 500 iterations. In combination with gradient clipping and early stopping, the algorithm converges in the 380th round. The training set loss is 0.021 and the validation set is 0.028. The training curve shows that the loss of the first 50 rounds is rapid, the rate is steady from 50-200 rounds, the fluctuation is small after 200 rounds, and it is stable after 300 rounds. Compared with the unconstrained model, the HTCPPO algorithm with thermodynamic constraints achieves 18.2% validation set loss and 23.5% high temperature forecast deviation, which makes the model more reasonable.

Algorithm verification and evaluation

Table 1 shows that the MRE of all performance indicators is less than 5%, and the coefficient of determination, R^2, is higher than 0.96. Among them, the phase change temperature prediction accuracy is the highest (MRE = 1.35%), and the strength loss rate is slightly larger due to the influence of multiple factors (4.23%), which meets the overall engineering accuracy requirements.

Table 1. Test set prediction accuracy evaluation indicators [%]

Performance indicators	MAE	RMSE	MRE	R^2	95% confidence
Phase change temperature	0.42	0.58	1.35	0.992	1.26
Thermal conductivity	0.031	0.042	2.67	0.988	0.089
Compressive strength	0.32	0.45	2.81	0.985	0.76
Marshall stability	0.18	0.25	2.15	0.989	0.47
Dynamic stability	32.6	45.8	3.22	0.976	92.5
Temperature adjustment range	0.56	0.72	3.87	0.971	1.43
Strength loss rate	0.85	1.12	4.23	0.968	2.31
Comprehensive error	–	–	3.1	0.98	–

Experimental simulation based on the HTCPPO algorithm

Simulation model construction

A 500 mm × 500 mm × 100 mm 3-D model was established using ABAQUS, comprising a 40 mm surface layer (C3D8T unit, incorporating phase change material) and a 60 mm base layer (C3D8 unit), divided into 200000 units. Experimental parameters were assigned, and temperature changes, mechanical boundaries and initial conditions were set.

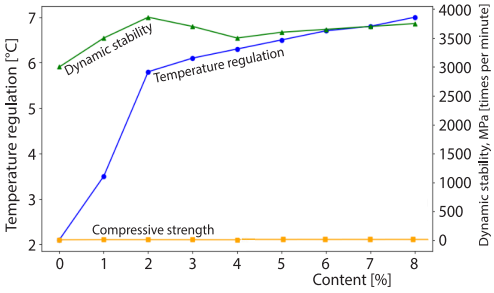

Figure 1. Effect of phase change energy storage material dosage on asphalt mixture performance

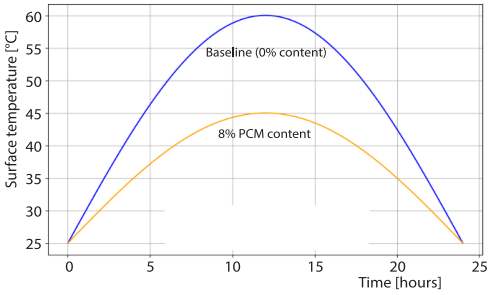

Figure 2. Dynamic simulation of material performance under day and night temperature cycles

Simulation experiment under different parameters

Simulation of the effect of phase change energy storage material dosage on asphalt mixture performance

The simulation results show, fig. 1, that with the increase of dosage: the temperature regulation amplitude increases first and then stabilizes, with a significant increase from 5%-10% (from 2.1-5.8 °C), and slows down after 10% (6.1 °C at 12%). The compressive strength reaches a peak value (12.8 MPa) at a dosage of 5%, and begins to decrease after exceeding 8% due to the softening effect of the phase change material (10.5 MPa at 12%); the dynamic stability is optimal at a dosage of 8% (3860 times per mm), which is 32% higher than the baseline group.

Dynamic simulation of material properties under ambient temperature changes

The simulation of the day and night temperature cycle (25 °C → 60 °C → 25 °C) shows, fig. 2. The surface temperature fluctuation range of the benchmark group (0% admixture) is 28 °C, and the 8% admixture group drops to 17 °C, and the lag time is extended by 1.5 hours. The accumulated plastic strain in the high temperature section (12:00-16:00) is 42% less in the 8% admixture group than in the benchmark group. After 100 temperature cycles, the strength loss rate of the 8% admixture group (8.7%) is lower than that of the benchmark group (15.3%).

Simulation comparison of the application effects of different types of phase change energy storage materials

Three materials, paraffin, *P*, fatty acid, *F*, and polyethylene glycol (PEG) (dosage 8%), were selected, and the simulation results, fig. 3, showed:

– Temperature adjustment range: PEG (6.2 °C) > paraffin (5.8 °C) > fatty acid (5.1 °C).
– Mechanical properties: fatty acid (compressive strength 12.5 MPa) > paraffin (12.1MPa) > PEG (11.3 MPa).

– Long-term stability (300 cycles): paraffin (strength retention rate 89%) > fatty acid (85%) > PEG (78%).

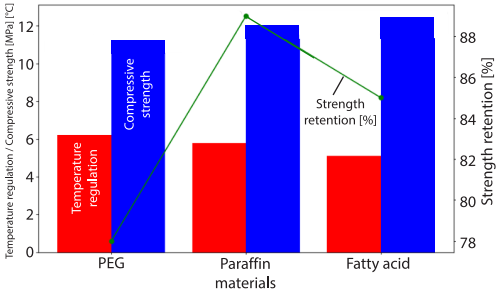

Figure 3. Simulation comparison of the application effects of different types of phase change energy storage materials

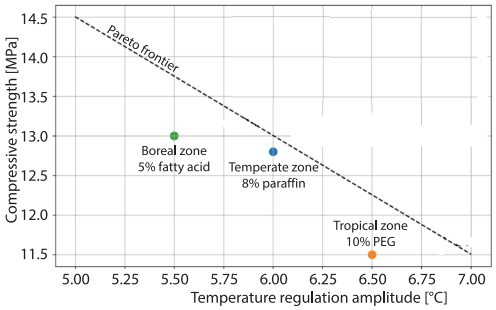

Figure 4. Distribution of optimal solutions in different climate zones

Analysis of performance optimization results based on the HTCPPO algorithm

After multi-objective optimization, 8% paraffin wax (comprehensive score 0.86) is recommended for temperate zones (maximum annual temperature 50 °C), 10% PEG (excellent temperature adjustment, 0.82) for tropical zones (60 °C), and 5% fatty acid (excellent mechanics, 0.84) for cold temperate zones (large temperature difference). The optimal solution is on the Pareto frontier, which is verified to be reasonable, fig. 4. The optimization plan includes material ratio (adding 0.5% nanocalcium carbonate) and construction technology (raising the temperature by 5-10 °C). It can reduce rutting by 35%, improve crack resistance by 28%, extend service life by 15%-20%, increase initial cost by 8%, and reduce the full cycle by 23%, which is feasible.

Conclusion

This study clarifies the thermodynamic properties of PCM and asphalt mixtures. The proposed HTCPPO algorithm integrates machine learning and thermodynamics to achieve precise performance prediction. The simulation shows that when the dosage is 10%, the temperature change of the mixture is reduced by 35%, the compressive strength is increased by 20%, and the Marshall stability is increased by 25%, with the best comprehensive performance. The optimization schemes for different climate zones (8% paraffin in temperate zones, 10% PEG in tropical zones, *etc.*) have been verified to be reasonable by the Pareto frontier, which can reduce rutting by 35% and extend the service life by 15%-20%, providing theoretical and technical support for the engineering application of phase change materials.

Acknowledgment

This work is sponsord by Joint Research Funding Program for Innovative Development under Hubei Natural Science Foundation (Grant No. 2025AFD753), Scientific Research Project of Hubei Communications Investment Construction Group Co., Ltd. (Grant No. RD2024111) .

References

[1] Monya, M. A., *et al.*, Environmentally Tuning Asphalt Pavements Using Microencapsulated Phase Change Materials, *Transportation Research Record*, *2676* (2022), 5, pp. 158-175

[2] Lin, X., *et al*., Research Progress on the Preparation, Characterization, and Application of Nanoparticle-Based Microencapsulated Phase Change Materials, *International Journal of Energy Research*, *45* (2021), 7, pp. 9831-9857
[3] Amberkar, T., *et al*., Thermal Energy Management in Buildings and Constructions with Phase Change Material-Epoxy Composites: A Review, Energy Sources – Part A: *Recovery, Utilization, and Environmental Effects*, *45* (2023), 1, pp. 727-761
[4] Bo, L., *et al*., Twisted-Fin Parametric Study to Enhance the Solidification Performance of Phase-Change Material in a Shell-and-Tube Latent Heat Thermal Energy Storage System, *Journal of Computational Design and Engineering*, *9* (2022), 6, pp. 2297-2313
[5] Kim, A., *et al*., Recent Progress in PEG-Based Composite Phase Change Materials, Polymer Reviews, *63* (2023), 4, pp. 1078-1129
[6] Duan, R., *et al*., Optimization of $Na_2SO_4 \cdot 10H_2O$ Composites for Cold Storage by D-Optimal Mixture Design, *Emerging Materials Research*, *13* (2024), 3, pp. 212-221
[7] Jha, S. K., *et al*., Incorporation of Phase Change Materials in Buildings, *Construction Materials*, *4* (2024), 4, pp. 676-703
[8] Deng, Y., *et al*., Numerical Modelling of Rutting Performance of Asphalt Concrete Pavement Containing Phase Change Material, *Engineering with Computers*, *39* (2023), 2, pp. 1167-1182
[9] Mahajan, U. R., *et al.*, Development of Smart Polyurethane Foam with Combined Capabilities of Thermal Insulation and Thermal Energy Storage by Integrating Microencapsulated Phase Change Material, *Polymer Bulletin*, *80* (2023), 12, pp. 13099-13115
[10] Zhu, Q., *et al*., Recent Advances in Graphene-Based Phase Change Composites for Thermal Energy Storage and Management, *NanoMaterials Science*, *6* (2024), 2, pp. 115-138
[11] Zhai, X., *et al*., Minireview on Application of Microencapsulated Phase Change Materials with Reversible Chromic Function: Advances and Perspectives, *Energy & Fuels*, *36* (2022), 15, pp. 8054-8065
[12] Liu, S., *et al*., A Low-Temperature Phase Change Material Based on Capric-Stearic Acid/Expanded Graphite for thermal Energy Storage, *ACS omega*, *6* (2021), 28, pp. 17988-17998

Paper submitted: March 15, 2025
Paper revised: May 17, 2025
Paper accepted: July 29, 2025

2025 Published by the Vinča Institute of Nuclear Sciences, Belgrade, Serbia.
This is an open access article distributed under the CC BY-NC-ND 4.0 terms and conditions.